Marine Micropaleontology 143 (2018) 70–79

Contents lists available at ScienceDirect

Marine Micropaleontology

journal homepage: www.elsevier.com/locate/marmicro

Research paper

Morphometry of the diatom *Fragilariopsis kerguelensis* from Southern Ocean sediment: High-throughput measurements show second morphotype occurring during glacials

Michael Kloster[a,b,*], Gerhard Kauer[b], Oliver Esper[a], Nike Fuchs[a], Bánk Beszteri[a]

[a] Alfred-Wegener-Institut Helmholtz-Zentrum für Polar- und Meeresforschung, Am Handelshafen 12, 27570 Bremerhaven, Germany
[b] Hochschule Emden/Leer, Constantiaplatz 4, 26723 Emden, Germany

ARTICLE INFO

Keywords:
Paleoceanography
SHERPA
Proxy
Valve area
Rectangularity
Holocene

ABSTRACT

Fragilariopsis kerguelensis is one of the most abundant diatoms in the sediments of the Southern Ocean. Its morphometric features have been proposed as proxies, based on links with, for example, iron availability, sea surface temperature and glacial/interglacial conditions. We investigated morphometric changes in *F. kerguelensis* valves in a well-studied sediment core record, focusing on transition periods between glacials and interglacials. By applying a high-throughput diatom imaging and morphometry workflow, we found two clearly distinct morphotypes which were differentiated by their rectangularity. One of them occurred preferentially in glacial samples, whilst the other persisted throughout. This indicates that their relative abundances depend on environmental conditions and thereby points to the possibility that paleo-proxies based on *F. kerguelensis* valve morphometric features might in the future benefit from differentiating these two morphotypes. As an initial exploration of this idea, we show that the abundance ratio of both morphotypes correlates well with paleo-temperatures which had been reconstructed using independent data from the same core. Distinguishing between the two morphotypes only became possible by image analysis for precisely measuring diatom valve outlines and area, highlighting the potential of such methods for diatom analyses.

1. Introduction

The siliceous sediment below large areas of the Southern Ocean contains a diatom record which has extensively been used for paleoceanographic reconstructions (Gersonde et al., 2005; Abelmann et al., 2006; Crosta, 2009; Shukla et al., 2009). Reconstructions of paleo-temperatures and of sea ice cover are mostly performed using transfer functions which link taxonomic composition of sediment assemblages to environmental variables (Zielinski et al., 1998; Gersonde et al., 2003; Crosta et al., 2004; Esper and Gersonde, 2014a; Esper and Gersonde, 2014b). But observations of intraspecific morphometric variation correlated with environmental conditions have also led to ideas to use such intraspecific variability to learn about past oceanographic conditions (Cortese and Gersonde, 2007; Nair et al., 2015; Shukla et al., 2016; Shukla and Crosta, 2017). Most attention in this regard was directed at marine diatom species *Fragilariopsis kerguelensis* (O'Meara) Hustedt (Hasle, 1965) which is, at least in terms of valve counts, the most abundant diatom species in Southern Ocean sediments (Abelmann and Gersonde, 1991; Warnock et al., 2015; Shukla et al., 2016). Variation in quantitative characters like valve length, width and area, as well as striation density, and the composite descriptor F or F* (Eq. (3)), were proposed to be related to productivity, iron availability, (summer) sea surface temperature, the position of the Antarctic Polar Front and to glacial/interglacial regimes (Fenner et al., 1976; Cortese and Gersonde, 2007; Cortese et al., 2012; Shukla et al., 2013; Shukla and Crosta, 2017). The reliability of these proxies is still under discussion, because *F. kerguelensis* has a highly variable valve morphology (Hasle, 1965), which can be affected by multiple, partly intercorrelated causes (Crosta, 2009; Cortese et al., 2012; Shukla et al., 2013; Shukla and Crosta, 2017), but it seems clear that morphometrics of valves of this diatom species are affected by environmental conditions.

In this study, the question was asked whether precise measurement

Abbreviations: λ, mixing proportion; df, degrees of freedom; MIS, marine isotope stage; μ, mean; n, sampling size; p, p-value; r, Pearson Correlation Coefficient; R^2, square of r; σ, standard deviation; SSST, summer sea surface temperature

* Corresponding author at: Alfred-Wegener-Institut Helmholtz-Zentrum für Polar- und Meeresforschung, Am Handelshafen 12, 27570 Bremerhaven, Germany.
E-mail addresses: michael.kloster@awi.de (M. Kloster), gerhard.kauer@hs-emden-leer.de (G. Kauer), Oliver.Esper@awi.de (O. Esper), bank.beszteri@awi.de (B. Beszteri).

https://doi.org/10.1016/j.marmicro.2018.07.002
Received 23 January 2018; Received in revised form 10 July 2018; Accepted 11 July 2018
Available online 12 July 2018

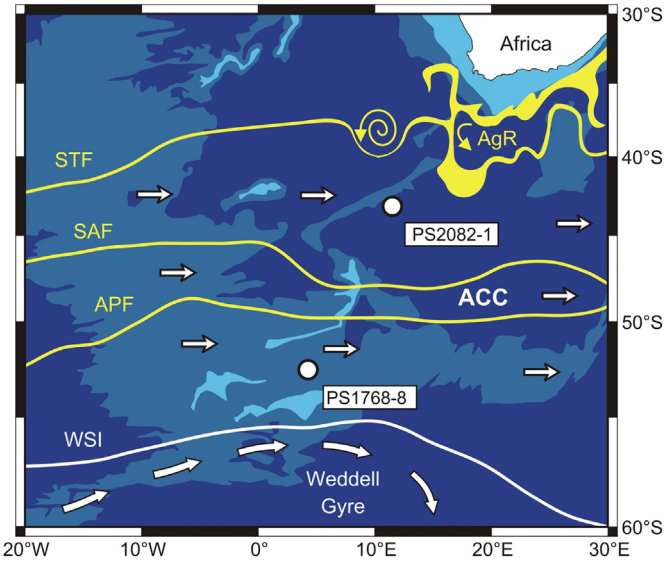

Fig. 1. Oceanographic setting of the coring site PS1768–8. ACC = Antarctic Circumpolar Current, AgR = Agulhas retroflection region, APF = Antarctic Polar Front, SAF = Subantarctic Front, STF = Subtropical Front, WSI = winter sea ice edge.

of valve outline features using a semi-automated procedure (Kloster et al., 2014; Kloster et al., 2017) might provide novel insights on this intraspecific morphometric variability. For this we analyzed material from the previously well investigated Southern Ocean sediment core PS1768–8 (Gersonde and Hempel, 1990; Gersonde, 2003), which was taken close to the average position of the Antarctic Polar Front (APF, Fig. 1). The use of a partially automated workflow (Kloster et al., 2017) enabled us to process large sample sizes (mostly between ca. 300 and 1000 valves per sample), and to assess a broad range of morphometric features. Observing distributions of diverse morphometric descriptors, we found that the *F. kerguelensis* "populations" in some layers of this sediment core consisted of two morphotypes, separated by the morphometric descriptor rectangularity (Droop, 1995). In this paper, we describe these findings and the occurrence of these morphotypes over two glacial to interglacial transitions in the core, and provide an initial exploration of whether their relative abundances might become useful for developing novel paleo-proxies.

2. Material and methods

The sediment core was obtained and processed for diatom analyses as described in Zielinski (1993). Valve densities on the original slides used by Zielinski (1993) were high. Since this caused difficulties for automated analysis, we re-mounted oxidized material at lower densities. This was done by drying ca. 1 ml diluted valve suspension onto cover slips in 12-well cell culture plates and embedding in Naphrax. Sampling depths were chosen with emphasis on transitions between glacial and interglacial periods (Table 1).

Valve outline features were quantified with the diatom morphometry software SHERPA (Kloster et al., 2014), applying the workflow and methods described in Kloster et al. (2017). This procedure includes two automated microscopic imaging steps: the first one is an area scan (creating a "panorama image" of the slide) performed at a low magnification/low resolution which is used to locate valves of interest on the slide. The second imaging step revisits only the positions where valves of interest were located, to image them by high resolution focus stacks. In more detail, first, a manually marked area of each slide was scanned with a low magnification objective (ZEISS Plan-Apochromat 10×/0.45 or ZEISS EC Plan-Neofluar 20×/0.5) in overlapping fields-of-view using a Metafer slide scanning system (MetaSystems,

Table 1
Basic information on samples analyzed from sediment core PS1768-8. Age and SSST estimates as well as assignment to marine isotope stages (MIS) following Esper and Gersonde (2014b).

Sampling depth (cm)	Index referring to Fig. 3	Age (yrs)	SSST (°C)	MIS	Sampling size
60	a	10,195	2.7	1	85
80	b	11,182	4.4	1	698
100	c	12,071	2.3	1	857
110	d	12,516	2.2	1	553
120	e	12,960	1.7	1	322
130	f	13,405	1.7	1	83
140	g	13,849	1.8	1	255
150	h	14,912	**0.9**	2	1659
160	i	16,130	**0.8**	2	1458
170	j	17,347	**0.6**	2	765
180	k	18,565	**0.8**	2	441
190	l	19,782	**0.5**	2	650
200	m	21,000	**0.8**	2	716
780	n	119,500	2.2	5	471
800	o	123,700	3.5	5	437
810	p	125,800	3.1	5	550
820	q	127,900	1.9	5	420
830	r	130,000	**0.7**	5	732
840	s	132,100	**0.7**	6	166
850	t	134,200	**0.5**	6	265
870	u	138,400	**0.6**	6	274
All depths combined					11,857

Sampling size: number of *Fragilariopsis kerguelensis* valves analyzed in the present study from the corresponding core depth. Reconstructed SSST ≤0.9 °C (glacial periods) is highlighted in bold letters.

Altlussheim, Germany; individual field-of-view images had 1360 × 1024 pixels at 1.55 pixels/µm for the 10× objective, 3.1 pixels/µm for the 20× objective). These images were analyzed with SHERPA to locate target valves. These positions were then imaged in a second scanning cycle with a 63× oil immersion objective (ZEISS Plan-Apochromat, N.A. = 1.40; again 1360 × 1024 pixels, at 9.8 pixels/µm) at 20 focus positions in 0.2 µm distances with the Metafer system. The 20 focus plane images were combined to produce an extended depth-of-focus image (performed as part of image processing by the Metafer image acquisition software). These high resolution extended depth-of-focus images were finally analyzed with SHERPA again, this time for precise morphometric characterization. During this step, every single valve considered by SHERPA was checked manually to make sure that it belongs to *Fragilariopsis kerguelensis*, and that segmentation of the valve outline was performed well by the software. If necessary, the valve outline was corrected manually. Morphometric descriptors were then saved from SHERPA for further data analysis and processing using R (R Core Team, 2015). Since the area scanned during the first low magnification step, as well as the sample density, determined the valves scanned during the second high magnification step, the amount of analyzed valves varied for each sample.

Low resolution area scans for core depths 800–820 cm were obtained using a 10× objective, for all other sampling depths a 20× objective was used. We switched to using the 20× objective when it became apparent that this reduced manual efforts when locating diatom valves in the first scanning cycle, without affecting the quality of results. Settings for SHERPA and employed shape templates are supplied in supplement "SHERPA settings". Data analysis was performed in R (R Core Team, 2015), the respective scripts can be found in supplement "Data". We modeled rectangularity distributions by a mixture of two univariate normal distributions, fitted by an expectation maximization algorithm (Benaglia et al., 2009).

Valve area measurements by SHERPA were performed by counting pixels lying within the segmented valve area; we will refer to these values as measured valve area. To compare these with literature values, which we will refer to as estimated valve area, we applied the equation

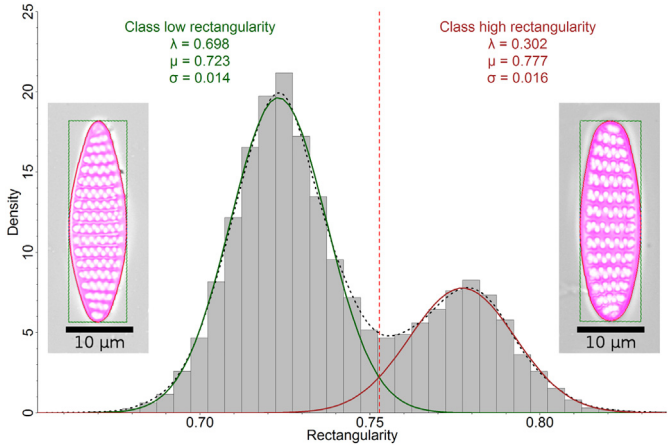

Fig. 2. Bimodal distribution of the morphometric descriptor rectangularity over all sampling depths. The gray bars show a histogram of all rectangularity values observed throughout the core, whereas the dotted black curve depicts their density estimate, i.e., a smoothed variant of the histogram. Solid curves depict the two component normal distributions resulting from fitting a mixture to the observed data; in green for the low and maroon for the high rectangularity class, with parameter values estimated given as text in the same colour as the corresponding curve (μ referring to the estimated mean, σ: standard deviation and λ: mixing proportion). The vertical dashed red line marks the threshold of 0.753 used to separate the two classes. Representative valves for each of the classes are shown on the left (lower rectangularity value, but a more lanceolate shape) and the right (higher rectangularity value, but a more elliptical shape). The valve area is highlighted purple and the surrounding rectangle is depicted in green (compare Eq. (2)). (For interpretation of the references to colour in this figure legend, the reader is referred to the web version of this article.)

given in (Shukla et al., 2013):

$$\text{Estimated valve area} = \text{apical length} * \text{transapical length} * 0.8 \quad (1)$$

The following morphometric descriptors were calculated using SHERPA (Kloster et al., 2014); the details here are only given for clarity: rectangularity was calculated as the ratio between the area of the valve and the area of the enclosing rectangle oriented parallel with the major axis of the valve (Droop, 1995, Fig. 2):

$$\text{Rectangularity} = \frac{\text{area of valve}}{\text{area of enclosing rectangle}} \quad (2)$$

F or F* was calculated according to Fenner et al. (1976); Cortese and Gersonde (2007):

$$F = F^* = \frac{\text{apical valve length}}{\text{transapical valve length}} \times \text{width of 5 costae} \quad (3)$$

Costae distance measurement is an experimental SHERPA feature. This frequency based method is mostly robust towards segmentation flaws, nevertheless results of costae distance ≥ 5 µm were assumed to be incorrect and thus rejected, which applied to ca. 0.5% of all data. The valve image was segmented by adaptive thresholding (Bradski and Kaehler, 2008), resulting in costae and valve border highlighted in white, whilst striae and image background were masked as black pixels. The segmented image was sampled along the central 80% of the valve's major (apical) axis by the Bresenham algorithm (Bresenham, 1965). Along this sampled line, each white section was replaced by a 5 pixel wide binomial-smoothed peak, resulting in an artificial 1d-image of costae positions. This was transformed into the frequency domain by discrete Fourier transform (DFT). Average costae distance was calculated from the frequency of the maximum magnitude of the Fourier transformed.

The strength of correlations, calculated by the Pearson correlation coefficient (r), is reported following the scheme Evans (1996) suggested (absolute values between 0.00 and 0.19 = very weak; 0.20–0.39 = weak; 0.40–0.59 = moderate; 0.60–0.79 = strong; 0.80–1.00 = very strong).

3. Results

We analyzed sediment core PS1768–8 by sampling 21 different depths, covering the past ca. 140,000 years, marine isotope stages (MIS) 1, 2, 5 and 6, and reconstructed SSST between 0.5 and 4.4 °C (Esper and Gersonde, 2014b; Abelmann et al., 2015), with emphasis on the transitions between glacial and interglacial periods. Morphometric features of ca. 12,000 valves were measured (Table 1); the data set is provided in supplement "Data".

3.1. Valve rectangularity

Combining measurements from all sampling depths, rectangularity (Eq. (2)) showed a clearly bimodal distribution (Fig. 2), which we approximated by fitting a mixture of two univariate normal distributions (Benaglia et al., 2009). In the following, we refer to these two distributions as classes of low and high rectangularity, marked by a green and a maroon curve, respectively. The low rectangularity class was defined by mean (μ) of ca. 0.72 and standard deviation (σ) of ca. 0.014, contributing ca. 70% (λ) of the valves over the whole core, with the valve shape being more lanceolate. The high rectangularity class had a μ of ca. 0.78, a σ of ca. 0.016, and contributed ca. 30% of all valves investigated, where the valve shape was more elliptical. Since the tails of both component distributions overlap, intermediate rectangularity values (roughly in the range between 0.73 and 0.77) cannot be unequivocally assigned to one of them. Nevertheless, for simplicity, we used a threshold of 0.753 to distinguish between them, corresponding to the point where the posterior probability of an observation belonging to either class is equal in the normal mixture model (Fig. 2). A more precise estimation of the contribution of both morphotypes to any single sample/population is possible by fitting the normal mixture with fixed μ and σ and optimizing the value of λ to the individual distribution, as illustrated in Fig. 4, but to avoid confusion, we only report the values from the simpler, threshold-based estimates in the following text unless stated otherwise.

Rectangularity distributions from individual sampling depths displayed different patterns (Fig. 3), appearing either uni- or bimodal; two extreme examples are given in Fig. 4, distributions for each of the sampling depths in Fig. A1 in supplement "Two rectangularity classes for each sampling depth". Valves from the low rectangularity class comprised between ca. 50% and nearly 100% of the *Fragilariopsis kerguelensis* populations (Fig. 5). The high rectangularity class preferentially occurred in core depths corresponding to reconstructed SSST values ≤ 0.9 °C (Fig. 3 blue colour), and contributed up to 50% of valves measured. For layers with the reconstructed value of SSST lying ≥ 1.7 °C (Fig. 3 red colour), the high rectangularity class contributed < 15% with a single exception (33% for 110 cm sampling depth, Fig. 5). SSST between 0.9 °C and 1.7 °C was not covered by our samples.

The relative contribution of both rectangularity classes varied across investigated core depths (Fig. 5). Samples from MIS 6 showed a much lower contribution of the high rectangularity class than samples with similar reconstructed SSST values from MIS 2. During the last glacial-interglacial transition, the high rectangularity class contributed exceptionally strongly at 110 cm sampling depth compared to nearby SSSTs. This signal might perhaps be related to the Antarctic Cold Reversal event (Cortese and Gersonde, 2007), although the paleo-temperatures reconstructed for the core do not show a cooling in this period. Apart from these cases, a general trend of increased contribution of the high rectangularity class in glacial intervals, i.e. at low reconstructed SSST values, could be observed.

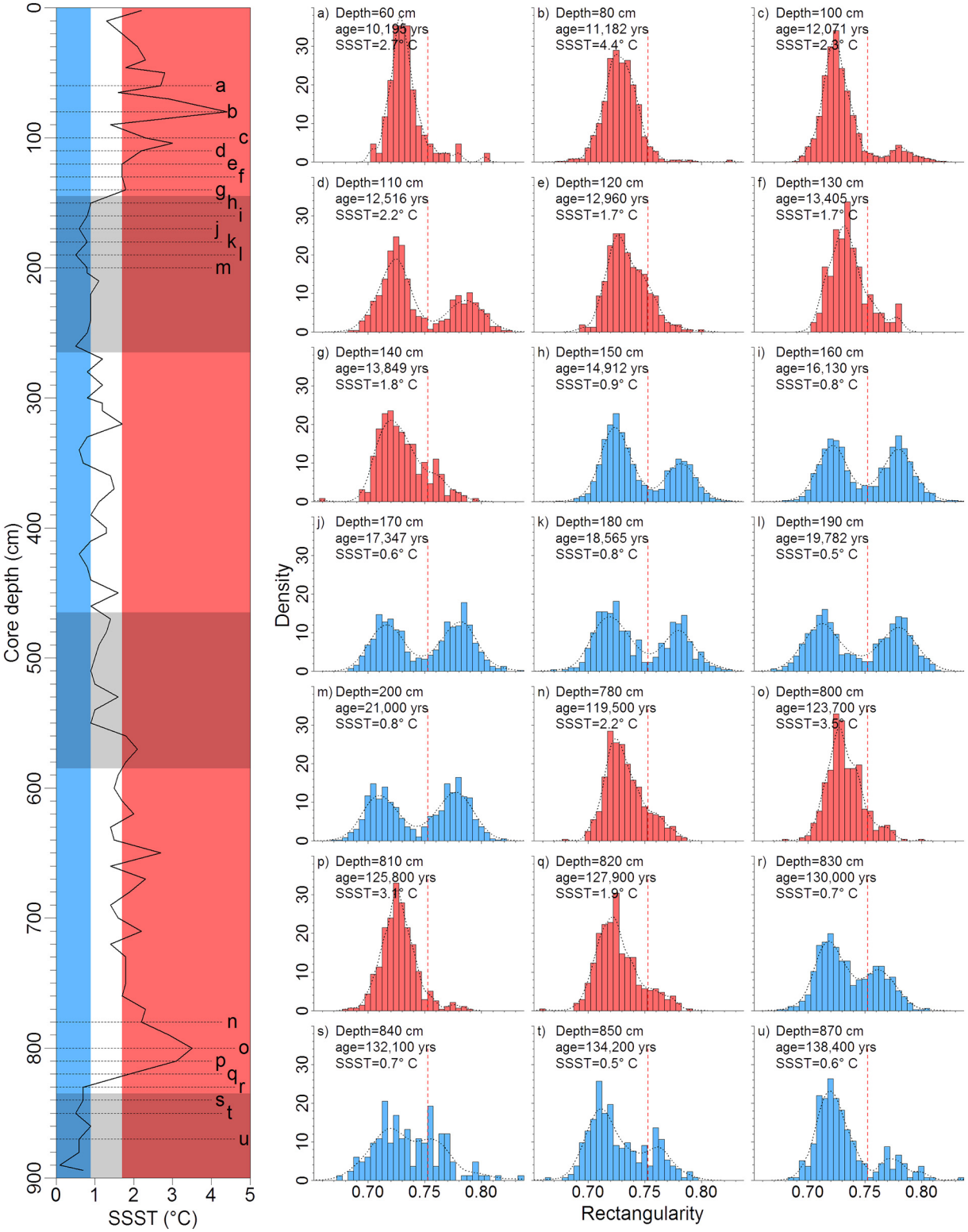

Fig. 3. Depth/age assignment and reconstructed paleoenvironmental information for core PS1768–8 in relation to valve rectangularity. Left: depth of core related to SSST, after Esper and Gersonde (2014b). Horizontal dotted lines mark the sampling depths we investigated, referred to by letters a to u. Shaded areas in the left hand panel indicate glacial periods according to MIS. Right: rectangularity histograms, a) – u) refer to the different sampling depths as indicated in the left hand panel and in Table 1. SSST ≤0.9 °C is marked in blue, ≥1.7 °C in red colour. Vertical dashed red lines in the histograms mark the threshold of 0.753 we used for separating the two rectangularity classes; the dotted black curves give a continuous representation of the distribution of observed rectangularity values in the form of density estimates. (For interpretation of the references to colour in this figure legend, the reader is referred to the web version of this article.)

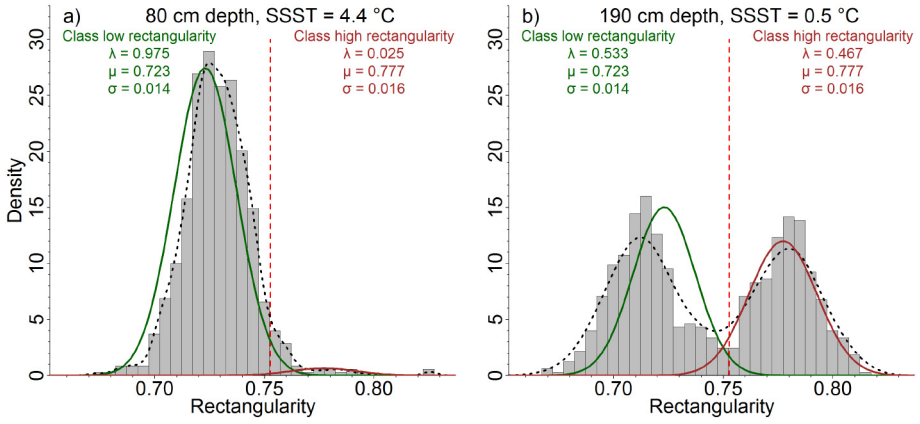

Fig. 4. Exemplary rectangularity histograms showing strongly differing contributions of rectangularity classes for a) 80 cm and b) 190 cm core depth. Dotted black lines show density estimates of the distribution of observed rectangularity values, i.e. a continuous representation of the observed distribution. Green and maroon lines depict the component normal distributions fitted using a mixture model for the low and high rectangularity classes as defined in Fig. 2 (i.e., mean μ and standard deviation σ fixed to the values estimated using the full data set, mixing proportion λ estimated anew for the specific sample). The dashed red lines mark the threshold of 0.753 we used for separating the two rectangularity classes. (For interpretation of the references to colour in this figure legend, the reader is referred to the web version of this article.)

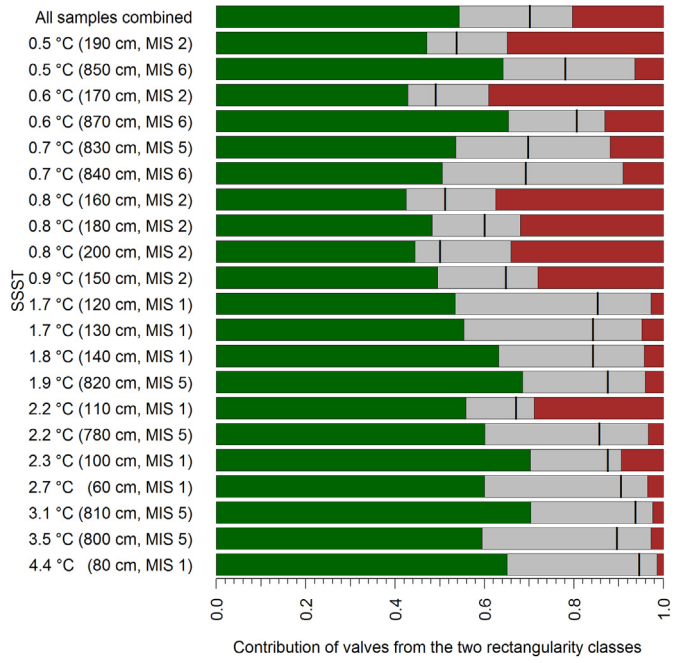

Fig. 5. Contribution of valves from the two rectangularity classes from different reconstructed SSSTs and sampling depths. The proportion of valves belonging to the low rectangularity class with a high confidence is shown in green, for the high rectangularity class in maroon. Gray colour marks the proportion of valves for which class assignment was uncertain, i.e. the posterior probability of belonging to one class differed from that of the other class by less than a factor of 100, according to the fitted mixture model. Black marks indicate the class border by a rectangularity threshold of 0.753. MIS 2 and 6 depict glacial, 1 and 5 interglacial periods. (For interpretation of the references to colour in this figure legend, the reader is referred to the web version of this article.)

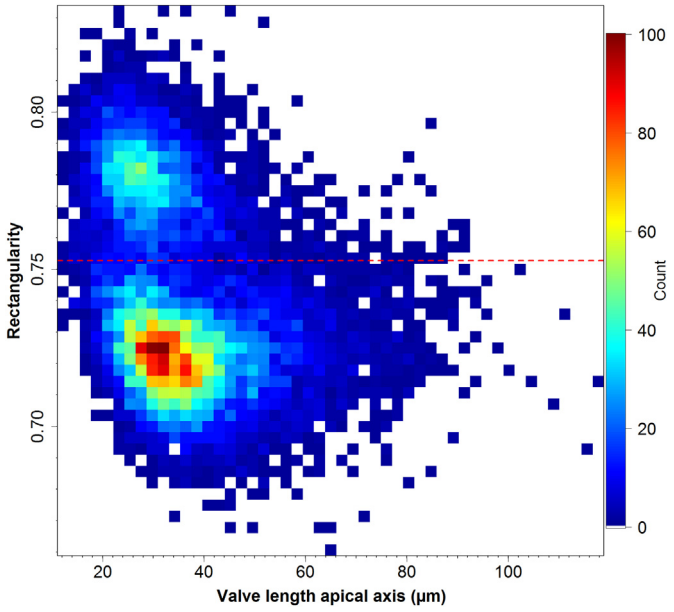

Fig. 6. Counts of valves of different rectangularity, compared to valve length, for measurements from all depths combined. The dashed red lines mark the threshold of 0.753 we used for separating the two rectangularity classes. (For interpretation of the references to colour in this figure legend, the reader is referred to the web version of this article.)

3.2. Rectangularity compared to valve length distribution

Since in *Fragilariopsis kerguelensis*, like in most other diatoms with elongate valves, valve outline shape changes accompany size decrease, rectangularity could depend on size. In that case, the presence of two somewhat distinct size classes could explain the bimodal rectangularity distributions observed. To test this possibility, the joint distribution of rectangularity and valve length was plotted (Fig. 6) which clearly showed that this was not the case. The two peaks present in the joint distribution appeared at similar valve lengths (around 25–30 μm), and were separated clearly on the rectangularity axis. Thus, we can exclude a bimodal size distribution as an explanation of the bimodal rectangularity distributions, as well as the possibility that the observed rectangularity differences represent valve shape changes related to the life cycle.

3.3. Further morphometric differentiation between rectangularity classes

To see if valves assigned to the low vs. high rectangularity class show any further morphometric differences, we compared further features between them and with their overall means (i.e. both rectangularity classes combined). Mean and median valve length in the high rectangularity class was found to be substantially lower than in the low rectangularity class (Table 2; also see Fig. 6). Similar observations could be made for valve width and area. In costae distance (striae density) however, both classes were virtually identical, and in F/F* differences were minor.

3.4. Correlation between valve area and SSST

Since it has been proposed that mean valve area of *Fragilariopsis kerguelensis* is related to sea surface temperature, the question arises if this relationship still holds for both rectangularity classes individually. Fig. 7 indicates that this is indeed the case: in the low rectangularity class, mean valve area correlated well with SSST ($R^2 = 0.348$, $r = -0.590$, df = 19; $p = .0049$ for the slope and $p < 2.2 \times 10^{-16}$ for the intercept). For the high rectangularity class as well as for the pooled

Table 2
Morphometric features, separated according to the two rectangularity classes.

Feature	Both rectangularity classes combined	Low rectangularity class	High rectangularity class
Rectangularity mean (µm)	0.74	0.72 (−2.2%)	0.78 (+5.24%)
Length mean (µm)	36.04	38.33 (+6.4%)	**30.63 (−14.99%)**
Length median (µm)	33.44	35.67 (+6.6%)	**28.77 (−13.98%)**
Width mean (µm)	9.15	9.56 (+4.5%)	**8.18 (−10.61%)**
Area mean (µm^2)	250.96	272.17 (+8.4%)	**200.96 (−19.92%)**
Costae distance mean (µm)	1.91	1.92 (+0.1%)	1.91 (−0.24%)
F or F* mean (µm)	37.79	38.59 (+2.1%)	35.90 (−4.99%)

Differences compared to values from both rectangularity classes combined are in brackets; differences ≥10% absolute are marked in bold letters.

data, correlation between mean valve area with SSST was only weak and not significant ($R^2 = 0.076$, $r = 0.276$, $p = .2253$ for the high rectangularity class; $R^2 = 0.044$, $r = -0.211$, $p = .359$ for the pooled data).

Our observations so far indicate that the relative contribution of both morphotypes reflects paleotemperature in the studied sediment core. To quantify this interrelationship, we regressed SSST against the ratio of rectangularity classes defined as

$$\text{Ratio of rectangularity classes} = \frac{\text{number of valves with rectangularity} \leq 0.753}{\text{number of valves with rectangularity} > 0.753} \quad (4)$$

A linear regression (Fig. 8) shows that this quantity is indeed a good predictor of reconstructed SSST values for this core, explaining around 80% of variability in reconstructed paleotemperatures.

4. Discussion

We investigated valve morphometric changes in *Fragilariopsis kerguelensis* valves in a well-studied sediment core record. Unexpectedly, we found two clearly distinct classes, differentiated by their rectangularity. In spite of the small relative difference (only ca. 7%) between both classes and of their overlap, they lead to clearly bimodal distributions in many individual core depths, as well as over the whole sediment core (Figs. 2–4). Means of some size-related morphometric features (valve length, width and area) were substantially different between both classes, but neither striae density nor F/F* were (Table 2). Proportion of valves matching these two classes varied between sampling depths of sediment core PS1768-8 (Figs. 3 & 4). Furthermore, we observed that differentiating *F. kerguelensis* low rectangularity morphotype leads to an improved correlation between valve area and reconstructed summer sea surface temperature (Fig. 7).

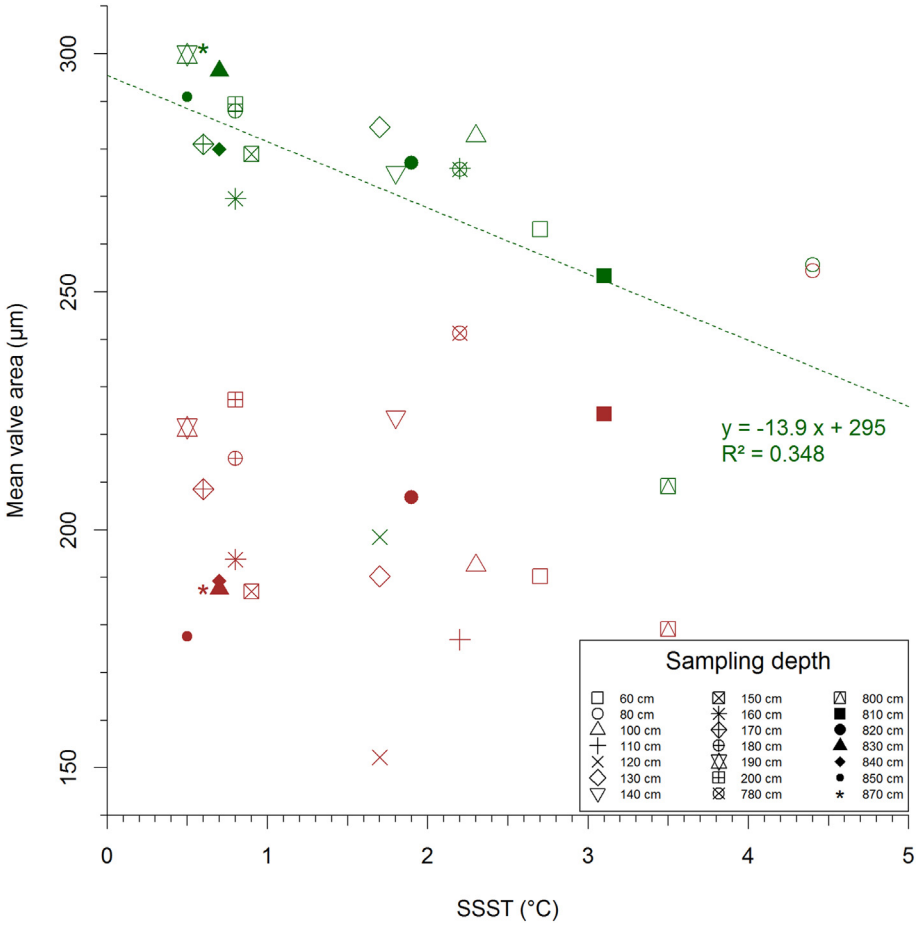

Fig. 7. Comparison of mean valve area and SSST, for low rectangularity class (green) and high rectangularity class (maroon); sampling depths are depicted by the indicated symbols. Ca. 35% of the variability in mean valve area within the low rectangularity class can be explained by a linear correlation to SSST (dashed green line), and < 8% for the high rectangularity class mean area (not shown). (For interpretation of the references to colour in this figure legend, the reader is referred to the web version of this article.)

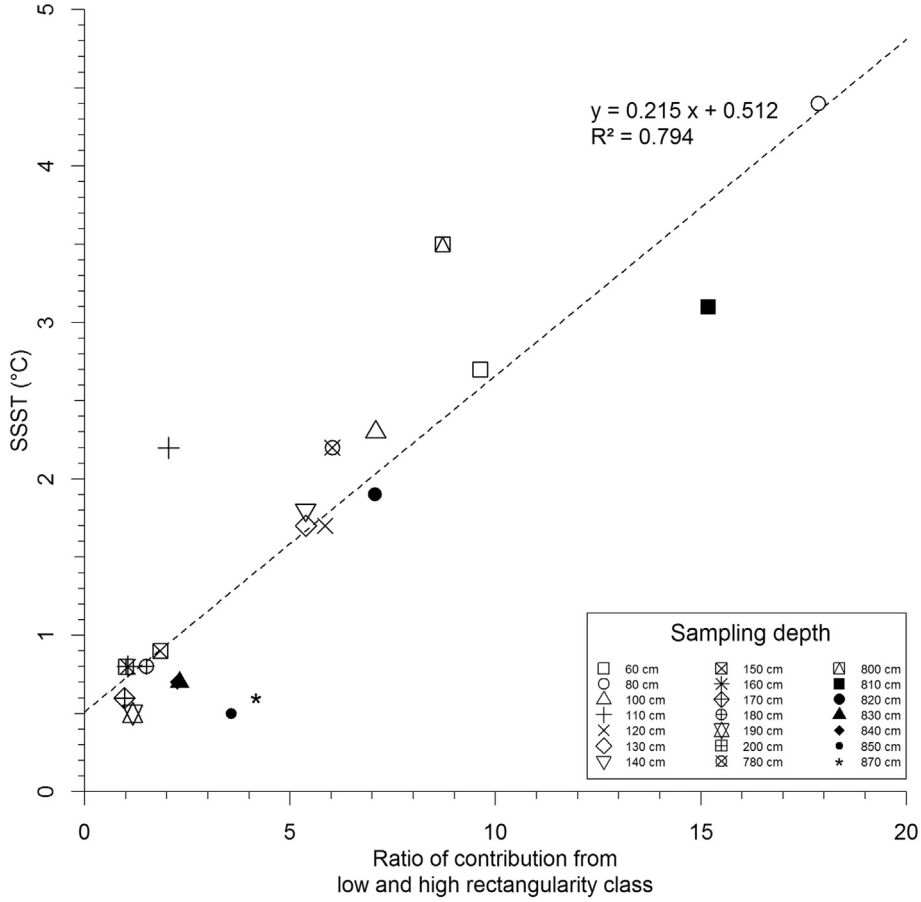

Fig. 8. Correlation between ratio of contribution from the two rectangularity classes (Eq. (4)) and SSST. Ca. 80% of the SSST variability can be explained by a linear correlation with the ratio (dashed line). The corresponding data is given in Table A1 in Supplement "Contribution from the two rectangularity classes".

4.1. Morphotypes distinct by rectangularity

Fragilariopsis kerguelensis morphology, as well as material from sediment core PS1768–8, has already been investigated thoroughly. Nevertheless, the two classes of different rectangularity we found herein (Fig. 2) have not been recognized before.

This is not necessarily surprising when considering that whenever both classes were clearly visible, also transitional forms, covering the whole rectangularity range between them, were present. In morphological taxonomy, the presence of a range gap or discontinuity in morphological variability is a commonly applied criterion for differentiating taxa (Mann, 1999); using this criterion, both rectangularity classes should indeed not be separated. Yet, rectangularity distributions appeared strongly bimodal in several individual sampling depths, as well as for all valves observed throughout the sediment core, clearly indicating that we are not dealing with a single homogeneous group of morphologies.

A shape transition from lanceolate towards elliptic valve outlines can often be observed as a result of size reduction in pennate diatoms (Woodard et al., 2016). Contrasting this, in our case the heterogeneity in rectangularity is not related to valve length, since valves belonging to both rectangularity classes can be observed at identical valve lengths (Fig. 6). Based on this, the variation in valve shapes captured by the rectangularity values cannot be explained by life cycle related shape change. To further illustrate this point, we show examples of valves belonging to both rectangularity classes at comparable sizes in Fig. 9. Valves from the low rectangularity class (Fig. 9a) exhibit a more lanceolate to shape and pointed apices. In contrast, valves from the high rectangularity class (Fig. 9b) have rounded apices, resulting in a more elliptical shape. This distinction can be observed throughout the whole size range.

The observed morphological variants might correspond to two different taxa, that is, groups of populations which are either reproductively isolated, or in reproductive contact, but under strong divergent selection upon their valve morphologies. Another possibility is phenotypic plasticity, that is, it is possible that *F. kerguelensis* cells can (possibly depending on environmental conditions, for example, temperature) switch their valve outline shapes from lanceolate to elliptic. Which of these possibilities applies to the *F. kerguelensis* valves with different rectangularity, cannot be decided based on only fossil material but needs information from cultures or molecular markers. For this reason, we will refer to these variants as morphotypes for the time being, until the biological nature of their difference has been clarified. In the following text, we will call the low rectangularity class morphotype I and the high rectangularity class morphotype II.

We now address whether these morphotypes correspond to taxa proposed previously. Donahue (1970) proposed *Nitzschia kerguelensis* var. *ovalis* (*N. kerguelensis* being synonymous with *F. kerguelensis*), documented by six valve images. Judging by its name, one could hypothesize that this variety corresponds to the more elliptical morphotype II we observed. We digitized and analyzed with SHERPA Donahue's published images of her var. *ovalis*, resulting in rectangularity ranging from 0.70 to 0.72. These values are at the lower side of the distributions for our low rectangularity class, depicting the more lanceolate morphotype I. She further reported a higher abundance of the proposed var. *ovalis* north of the Antarctic Convergence. This is also in contrast with our findings that morphotype II is abundant mostly at temperatures at the lower end of *F. kerguelensis* physiological

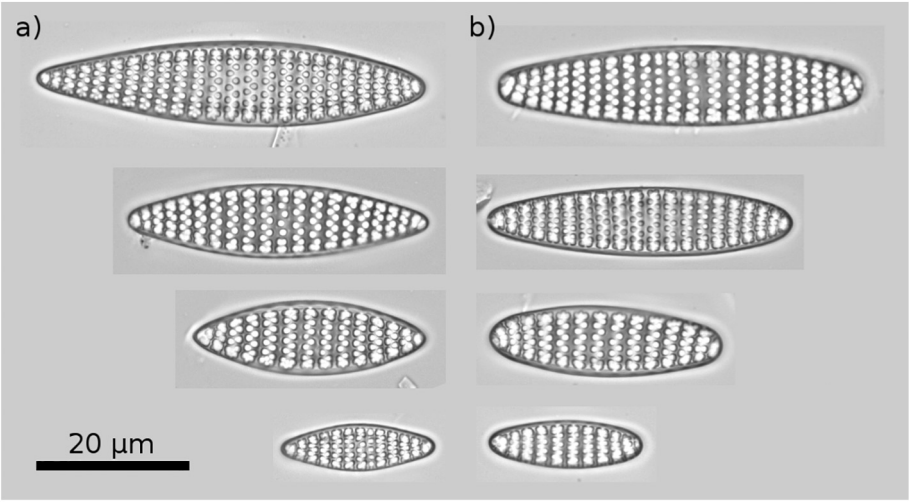

Fig. 9. Examples of the two Fragilariopsis kerguelensis morphotypes. a) morphotype I with pointed apices and more lanceolate shape. b) morphotype II with rounded apices and more elliptical shape. Valve lengths are ca. 50, 40, 30, 20 µm from top to bottom.

temperature range. Accordingly, we conclude that the *Nitzschia kerguelensis* var. *ovalis*, as proposed by Donahue (1970), is not congruent with the *F. kerguelensis* morphotype II we found, but with morphotype I.

Frenguelli (1960) also described an elliptically shaped variant in this species as *Fragilariopsis antarctica* var. *elliptica* (*F. antarctica* being synonymous with *F. kerguelensis*). However, this variety was rejected by Hasle (1965) because she observed that more elliptical valves usually occurred at lower sizes, and was of the opinion that this resulted from allometric change in valve outline shape. Cefarelli et al. (2010) agreed, since for Frenguelli's material they "*found a close correlation between form and valve size*". Our study is the first where the question of correlation between size and valve outline shape in *F. kerguelensis* is addressed quantitatively.

Although we indeed observed a negative correlation between rectangularity and valve length ($R^2 = 0.098$, $r = -0.313$, df = 11,855, $p < 2.2 \times 10^{-16}$), we clearly illustrated above (Figs. 6, 9) that the two morphotypes both occur at comparable sizes, i.e., they cannot be explained as valve shape change brought about by size diminution. From the single valve drawing which Frenguelli (1960) used to illustrate *F. antarctica* var. *elliptica*, we measured a rectangularity value of 0.78, which conforms to the more elliptical morphotype II we found. Cefarelli et al. (2010) presented further light microscopic images from Frenguelli's original material, from which we also measured rectangularity with SHERPA. One of two var. *elliptica* examples had a rectangularity of 0.769, which matches the high rectangularity class well, but this measurement might be imprecise due to partly defocused valve edges. However, the other example of var. *elliptica*, as well as the three *F. kerguelensis* var. *kerguelensis* examples, were within the overlapping range of the two rectangularity classes (0.746–0.758), so their class assignment is ambiguous. Nevertheless, at Frenguelli's sampling site (under ice near Port Martin winter station, Adélie Land at 66°49′ S), a SSST < 0.9 °C can be expected, which conforms with increased abundance of morphotype II in our sediment core samples. Thus, it seems possible that the var. *elliptica* described by Frenguelli (1960) matches the morphotype II we found. In this case, our analyses can be taken as evidence against the arguments put forward by Hasle (1965) and Cefarelli et al. (2010) refusing the validity of Frenguelli's proposed variety. The cited authors were correct in pointing out both that intermediate forms between highly elliptical and clearly lanceolate valves can be found in this species, and that elliptical valves more frequently occur at low sizes. However, valves with intermediate values of rectangularity are rare compared to valves with high or low rectangularity; and this observation even applies when comparing valves at a fixed size. If eventually both morphotypes observed here were to be differentiated taxonomically, Frenguelli's taxon could be revived.

4.2. Correlation of Fragilariopsis kerguelensis valve properties with environmental conditions

For *Fragilariopsis kerguelensis,* different morphometric characters including valve area, valve length and the combined factor F or F* have been observed to depend on environmental conditions and proposed as potential paleoclimate proxies (Donahue, 1970; Fenner et al., 1976; Cortese and Gersonde, 2007; Cortese et al., 2012; Shukla et al., 2013; Nair et al., 2015; Shukla and Crosta, 2017; Shukla and Romero, 2018).

Our study might have implications for this application of *F. kerguelensis* morphometrics in multiple ways. First, using slide scanning combined with image analyses allows increasing sample sizes, and, probably even more important, a more precise measurement of morphometric characters apart from simple length measurements. One case in point is valve area: estimations according to Eq. (1) (Shukla et al., 2013) overestimated values compared to our direct measurements by ca. 9% on average (Table A2 in Supplement "Valve area"). This is not surprising when considering that the rectangularity from our measurements, having an overall mean of 0.74, corresponds to their correction-factor of 0.8. If this was a consistent bias across different samples or core depths, this would be no problem; however, due to varying contributions of the two morphotypes (Fig. 5) and their distinct rectangularity (mean 0.72 and 0.78), the bias affects valve area estimates from different communities to different extents, so that the difference between measured and estimated valve areas ranges from 7.64–10.76% across the samples investigated herein. Whether this loss of precision can be afforded will depend on the exact question asked, but in general we propose that, whenever feasible, actual measurement of valve area should be preferred over estimation based on measuring valve length and width only.

The second aspect with potential relevance for *F. kerguelensis* morphometric proxies is our finding of two different morphotypes. Regardless of whether both morphotypes correspond to distinct (sub-) species or to phenotypic variants of the same species, their relative occurrence shows a strong correspondence with paleo-environmental conditions, since the high rectangularity morphotype II occurred preferentially during glacial periods. Based on this, it is both possible that the relative contribution of both morphotypes might become useful as (part of) a paleoceanographic proxy, and that explicitly distinguishing both morphotypes might improve the precision or resolution of any one of the previously proposed *F. kerguelensis* morphometric proxies.

For the *F. kerguelensis* valve area proxy, a complex interpretation framework has emerged which takes into account deviation of water temperature from optimal values for the species, macronutrient and iron supply, species specific productivity, as well as oceanographic reorganizations and changing sea ice cover (Cortese and Gersonde, 2007; Crosta, 2009; Cortese et al., 2012; Shukla et al., 2013; Shukla and Crosta, 2017; Shukla and Romero, 2018). These studies have shown that characterizing morphometric variability in this species as latitudinal gradients, as originally proposed by Donahue (1970) or Fenner et al. (1976), is overly simplistic. For instance, valve area has its maximum in a band between the Polar Front and the seasonally ice covered zone, and decreases both to the South and North of this region (Cortese and Gersonde, 2007). In the present study, paleotemperature was used simply as an illustration because it is readily available, but it is clearly only one out of several important ecological determinants of patterns of morphometric variability within this species (or species complex). Going beyond the simple recognition of the existence of two morphotypes, as done herein, and to fully assess the consequences and potential uses of this fact for proxy development and application, will need a broader sampling focusing on recent material, from well characterized environmental settings. Besides this, applying precise measurements of a broader range of morphometric characteristics, i.e., going beyond valve area and rectangularity, might also provide complementary insights. Since this species is numerically so abundant in the Southern Ocean sediment, and is relatively easy to recognize and analyze, it has practical advantages and it might accordingly be a system for paleo-proxies that is worth to be still developed further in the future.

5. Conclusions

We found two morphotypes of *Fragilariopsis kerguelensis*, distinguished by characteristics of the valve apices, which appear to be either pointed, resulting in a more lanceolate valve shape, or more rounded, resulting in a more elliptical valve shape. This difference becomes apparent in the morphometric descriptor rectangularity, which indicates the presence of two clearly distinct classes for the material we investigated. Increased occurrence of the more elliptical morphotype was observed at lower reconstructed paleo-temperatures.

Whether these patterns results from the presence of so far unrecognized taxa within *F. kerguelensis* or from phenotypic plasticity, needs to be clarified using extant (living or DNA containing) samples. It is possible that differentiating between both morphotypes could improve existing paleo-proxies based on *F. kerguelensis* valve morphometric features, or could form the basis for novel ones; this question also needs to be addressed in follow-up studies using extant material from known environmental conditions.

Acknowledgements

This work was supported by the Deutsche Forschungsgemeinschaft (DFG) in the framework of the priority programme 1158 “Antarctic Research with comparative investigations in Arctic ice areas” (grant numbers BE4316/4-1, KA1655/3-1).

We would like to express our gratitude to Rainer Gersonde for supplying material from sediment core PS1768-8, as well as to Friedel Hinz, Sean Seegert, Sarah Olischläger, Fenina Buttler and Fabian Altvater for preparing material used in this study and in previous preliminary experiments.

Author contributions

Bánk Beszteri and Gerhard Kauer supervised the project. Oliver Esper contributed material samples and paleoceanographic background. Nike Fuchs conducted preliminary measurements which were instrumental for designing this study. All of the aforementioned persons contributed to the paper's content. Slide scanning, image analysis and measurements via SHERPA, data analysis and paper writing were performed by Michael Kloster.

Appendix A. Supplementary data

Supplementary data to this article can be found online at https://doi.org/10.1016/j.marmicro.2018.07.002.

References

Abelmann, A., Gersonde, R., 1991. Biosiliceous Particle-Flux in the Southern-Ocean. Mar. Chem. 35, 503–536. https://doi.org/10.1016/S0304-4203(09)90040-8.

Abelmann, A., Gersonde, R., Cortese, G., Kuhn, G., Smetacek, V., 2006. Extensive phytoplankton blooms in the Atlantic sector of the glacial Southern Ocean. Paleoceanography 21. https://doi.org/10.1029/2005pa001199.

Abelmann, A., Gersonde, R., Knorr, G., Zhang, X., Chapligin, B., Maier, E., Esper, O., Friedrichsen, H., Lohmann, G., Meyer, H., 2015. The seasonal sea-ice zone in the glacial Southern Ocean as a carbon sink. Nat. Commun. 6. https://doi.org/10.1038/ncomms9136.

Benaglia, T., Chauveau, D., Hunter, D.R., Young, D.S., 2009. mixtools: an R package for analyzing finite mixture models. J. Stat. Softw. 32, 1–29. https://doi.org/10.18637/jss.v032.i06.

Bradski, G., Kaehler, A., 2008. Learning OpenCV : Computer Vision with the OpenCV Library. O'Reilly, Sebastopol.

Bresenham, J.E., 1965. Algorithm for computer control of a digital plotter. IBM Syst. J. 4, 25–30. https://doi.org/10.1147/sj.41.0025.

Cefarelli, A.O., Ferrario, M.E., Almandoz, G.O., Atencio, A.G., Akselman, R., Vernet, M., 2010. Diversity of the diatom genus *Fragilariopsis* in the Argentine Sea and Antarctic waters: morphology, distribution and abundance. Polar Biol. 33, 1463–1484. https://doi.org/10.1007/s00300-010-0794-z.

Cortese, G., Gersonde, R., 2007. Morphometric variability in the diatom *Fragilariopsis kerguelensis*: Implications for Southern Ocean paleoceanography. Earth Planet. Sci. Lett. 257, 526–544. https://doi.org/10.1016/j.epsl.2007.03.021.

Cortese, G., Gersonde, R., Maschner, K., Medley, P., 2012. Glacial-interglacial size variability in the diatom *Fragilariopsis kerguelensis*: possible iron/dust controls? Paleoceanography 27. https://doi.org/10.1029/2011PA002187.

Crosta, X., 2009. Holocene size variations in two diatom species off East Antarctica: Productivity vs environmental conditions. Deep-Sea Res. I Oceanogr. Res. Pap. 56, 1983–1993. https://doi.org/10.1016/j.dsr.2009.06.009.

Crosta, X., Sturm, A., Armand, L., Pichon, J.-J., 2004. Late Quaternary sea ice history in the Indian sector of the Southern Ocean as recorded by diatom assemblages. Mar. Micropaleontol. 50, 209–223. https://doi.org/10.1016/S0377-8398(03)00072-0.

Donahue, J.G., 1970. Diatoms as Quaternary Biostratigraphic and Paleoclimatic Indicators in High Latitudes of the Pacific Ocean. Columbia University, New York.

Droop, S., 1995. A morphometric and geographical analysis of two races of *Diploneis smithii/D. fusca* (Bacillariophyceae) in Britain. In: Proceedings of the 13th International Diatom Symposium. Biopress Ltd, Bristol, pp. 347–369.

Esper, O., Gersonde, R., 2014a. New tools for the reconstruction of Pleistocene Antarctic sea ice. Palaeogeogr. Palaeoclimatol. Palaeoecol. 399, 260–283. https://doi.org/10.1016/j.palaeo.2014.01.019.

Esper, O., Gersonde, R., 2014b. Quaternary surface water temperature estimations: New diatom transfer functions for the Southern Ocean. Palaeogeogr. Palaeoclimatol. Palaeoecol. 414, 1–19. https://doi.org/10.1016/j.palaeo.2014.08.008.

Evans, J.D., 1996. Straightforward statistics for the behavioral sciences. Brooks/Cole Publishing Co., CA.

Fenner, J., Schrader, H., Wienigk, H., 1976. Diatom phytoplankton studies in the southern Pacific Ocean, composition and correlation to the Antarctic Convergence and its paleoecological significance. Initial Rep. Deep Sea Drill. Proj. 35, 757–813.

Frenguelli, J., 1960. Diatomeas y silicoflagelados recogidas en Tierra Adelia durante las Expediciones Polares Francesas de Paul-Emile Victor (1950-1952). Rev. Algol. 1, 3–48.

Gersonde, R., 2003. Documentation of Sediment Core PS1768-8. Alfred Wegener Institute - Polarstern Core Repositoryhttps://doi.org/10.1594/PANGAEA.108079.

Gersonde, R., Hempel, G., 1990. Die Expeditionen ANTARKTIS-VIII/3 und VIII/4 mit FS "Polarstern" 1989 = The expeditions ANTARKTIS VIII/3 and VIII/4 of RV "Polarstern" in 1989. Alfred Wegener Institute for Polar and Marine Research, Bremerhaven.

Gersonde, R., Abelmann, A., Brathauer, U., Becquey, S., Bianchi, C., Cortese, G., Grobe, H., Kuhn, G., Niebler, H.S., Segl, M., Sieger, R., Zielinski, U., Futterer, D.K., 2003. Last glacial sea surface temperatures and sea-ice extent in the Southern Ocean (Atlantic-Indian sector): A multiproxy approach. Paleoceanography 18. https://doi.org/10.1029/2002pa000809.

Gersonde, R., Crosta, X., Abelmann, A., Armand, L., 2005. Sea-surface temperature and sea ice distribution of the Southern Ocean at the EPILOG Last Glacial Maximum - a circum-Antarctic view based on siliceous microfossil records. Quat. Sci. Rev. 24, 869–896. https://doi.org/10.1016/j.quascirev.2004.07.015.

Hasle, G.R., 1965. *Nitzschia* and *Fragilariopsis* species studied in the light and electron microscopes. III. The genus *Fragilariopsis*. Skrifter utgitt av Det Norske Videnskaps-Akademi i Oslo, I. Matematisk-Naturvidenskapelig Klasse. Ny Serie 21, 1–49.

Kloster, M., Kauer, G., Beszteri, B., 2014. SHERPA: an image segmentation and outline feature extraction tool for diatoms and other objects. BMC Bioinforma. 15, 218. https://doi.org/10.1186/1471-2105-15-218.

Kloster, M., Esper, O., Kauer, G., Beszteri, B., 2017. Large-Scale Permanent Slide Imaging

and Image Analysis for Diatom Morphometrics. Appl. Sci. 7, 330. https://doi.org/10.3390/app7040330.
Mann, D.G., 1999. The species concept in diatoms. Phycologia 38, 437–495.
Nair, A., Mohan, R., Manoj, M., Thamban, M., 2015. Glacial-interglacial variability in diatom abundance and valve size: Implications for Southern Ocean paleoceanography. Paleoceanography 30, 1245–1260. https://doi.org/10.1002/2014PA002680.
R Core Team, 2015. R: A Language and Environment for Statistical Computing. R Foundation for Statistical Computing. https://www.R-project.org.
Shukla, S.K., Crosta, X., 2017. *Fragilariopsis kerguelensis* size variability from the Indian subtropical Southern Ocean over the last 42 000 years. Antarct. Sci. 29, 139–146. https://doi.org/10.1017/S095410201600050X.
Shukla, S.K., Romero, O.E., 2018. Glacial valve size variation of the Southern Ocean diatom *Fragilariopsis kerguelensis* preserved in the Benguela Upwelling System, southeastern Atlantic. Palaeogeogr. Palaeoclimatol. Palaeoecol. 499, 112–122. https://doi.org/10.1016/j.palaeo.2018.03.023.
Shukla, S.K., Mohan, R., Sudhakar, M., 2009. Diatoms: a potential tool to understand past oceanographic settings. Curr. Sci. 1726–1734.
Shukla, S.K., Crosta, X., Cortese, G., Nayak, G.N., 2013. Climate mediated size variability of diatom *Fragilariopsis kerguelensis* in the Southern Ocean. Quat. Sci. Rev. 69, 49–58. https://doi.org/10.1016/j.quascirev.2013.03.005.
Shukla, S.K., Crespin, J., Crosta, X., 2016. *Thalassiosira lentiginosa* size variation and associated biogenic silica burial in the Southern Ocean over the last 42kyrs. Mar. Micropaleontol. 127, 74–85. https://doi.org/10.1016/j.marmicro.2016.07.006.
Warnock, J.P., Scherer, R.P., Konfirst, M.A., 2015. A record of Pleistocene diatom preservation from the Amundsen Sea, West Antarctica with possible implications on silica leakage. Mar. Micropaleontol. 117, 40–46. https://doi.org/10.1016/j.marmicro.2015.04.001.
Woodard, K., Kulichová, J., Poláčková, T., Neustupa, J., 2016. Morphometric allometry of representatives of three naviculoid genera throughout their life cycle. Diatom. Res. 31, 231–242. https://doi.org/10.1080/0269249X.2016.1227375.
Zielinski, U., 1993. Quantitative Bestimmung von Paläoumweltparametern des Antarktischen Oberflächenwassers im Spätquartär anhand von Transferfunktionen mit Diatomeen = Quantitative estimation of palaeoenvironmental parameters of the Antarctic surface water in the Late Quaternary using transfer functions with diatoms. Universität Bremen.
Zielinski, U., Gersonde, R., Sieger, R., Fütterer, D., 1998. Quaternary surface water temperature estimations: Calibration of a diatom transfer function for the Southern Ocean. Paleoceanography 13, 365–383. https://doi.org/10.1029/98pa01320.